communications engineering

A Nature Portfolio journal

Viewpoint

https://doi.org/10.1038/s44172-026-00594-8

Editors' Choice 2025

By Pengfei Liu, Philip Coatsworth, Pedro Neto, Liangfei Tian, Cecilia de Carvalho Castro e Silva, Chaoran Huang, Rosamund Daw, Said Elias, Ali Behnood, Jonathon S. Schofield, Alessandro Rizzo, Or Perlman, Jordan Raney, Wan-Ting Grace Chen, Manabu Fujii, Danielle Densley Tingley, Wenjie Wang & Massimo Mastrangeli

The editorial team present a selection of highlights of research published in *Communications Engineering* in 2025

This year, we have selected twenty papers from different disciplines which tell fascinating research stories which we are excited to share again. They are presented in order of publication date from earliest to latest in the year. Please check our website for many more exciting research advances across the year.

Intelligent shipping: integrating autonomous manoeuvering and maritime knowledge in the Singapore-Rotterdam Corridor, Liang Zhao et al.

Maritime shipping, which accounts for over 80% of global trade by volume, faces persistent challenges in designing routes that are not only efficient but also inherently safe and reliable. Traditional route optimization methods often prioritize the shortest path or lowest cost, neglecting the specific operational preferences of shipping companies and, crucially, the real-world maneuvering characteristics of large vessels. This gap can lead to routes that are impractical to navigate or that elevate the risk of accidents. In their *Communications Engineering* paper[1], Liang Zhao and colleagues address this dual challenge by introducing an innovative model-data dual-driven framework that intelligently integrates maritime knowledge with autonomous maneuvering simulation.

The core of their methodology is a three-stage process that first processes historical automatic identification system data to extract high-quality vessel trajectories. It then employs an unsupervised hierarchical approach to mining maritime knowledge, revealing global patterns—such as seasonal variations and voyage durations—and local insights, including specific movement patterns, shipping behaviors, and traffic flow maps of major companies. This knowledge base allows for the design of customized routes that align with a company's unique requirements for departure season, voyage days, route preferences, and ports of call. The final and most distinctive stage involves a high-fidelity autonomous maneuvering model. This digital twin of a real ship incorporates non-linear hydrodynamics and an autonomous navigation system to simulate voyages along the designed routes, testing their safety and reliability before real-world deployment.

The researchers validate their framework on the world's longest Green and Digital Shipping Corridor between Singapore and Rotterdam. They successfully design and test two customized routes for the China Ocean Shipping Company (COSCO), demonstrating the system's flexibility in meeting specific corporate logistics. The autonomous maneuvering tests reveal how the model generates realistic courses and rudder commands, effectively navigating complex and narrow waterways like the Suez Canal. The resulting commands can be directly applied to ship autopilots or used to assist crew members, thereby reducing human error and enhancing navigational safety. This work stands out for its holistic approach, bridging the gap between large-scale data-driven planning and precise, physics-based ship control. It provides a foundational and highly practical step towards building fully digitalized platforms for the future of intelligent and autonomous shipping. *Pengfei Liu*

Periodic cooking of eggs, Emilia Di Lorenzo et al.

Eggs are an important foodstuff due to their range of functional properties and high nutritious value. However, they are a complex object to prepare "perfectly" due to their dual-material structure, consisting of a yolk within the egg white (also known as albumen). These two materials have different compositions and different optimal cooking temperatures: ~85 °C for albumen and ~65 °C for yolk. As a result, when the albumen has perfect consistency (as when hard-boiled), the yolk is dry and powdery. In contrast, when the yolk has perfect consistency, (as when prepared *sous vide*), the albumen is runny and liquid-like, as only one albumen protein (ovotransferrin) denatures at such low temperatures.

Emilia Di Lorenzo and colleagues developed a periodic cooking protocol, holding a shell-on egg in alternatively 100 °C and 30 °C water for 2-minute periods to cook both egg components at their ideal temperatures[2]. Initial simulations showed how heat transfer occurred under different cooking methods. Traditional boiling methods gave monotonic temperature increases, whereas periodic cooking was shown to have variable temperature behaviour: the albumen cycled between 100–87 °C and 30–55 °C during the hot and cold periods respectively, but the yolk was maintained at 67 °C. FTIR spectroscopic analysis of real cooked egg samples corroborated the degree of cooking estimations found for each technique via simulations, and confirmed that protein denaturation aligned with thickening and gelation. Quantitative descriptive analysis (an objective sensory analysis method) established that the sensory properties (e.g., visual, mouthfeel, flavour) of periodically cooked eggs typically corresponded to the most favourable properties from each of the other cooking methods (Fig. 1). Nutritional analysis also showed that periodically cooked eggs have a greater nutritional profile than traditional methods (such as a higher polyphenol content), as found through ^{1}H NMR and mass spectrometry analysis.

This paper caught my attention due to its relevance to "molecular gastronomy" or experimental cooking, but using a method that could easily be replicated in a domestic setting. Since publication, many people have tried out this method[3–5]. Its investigations into solving heat transfer problems have application in other engineering and material science areas too, such as in curing, crystallization, and structuring of materials. One specific area already investigated using similar techniques is the production of foams with layers of different morphologies or densities, achieved through manipulation of processing variables (such as pressure) under time-varying boundary conditions in mass transport of the blowing agents[6]. *Philip Coatsworth*

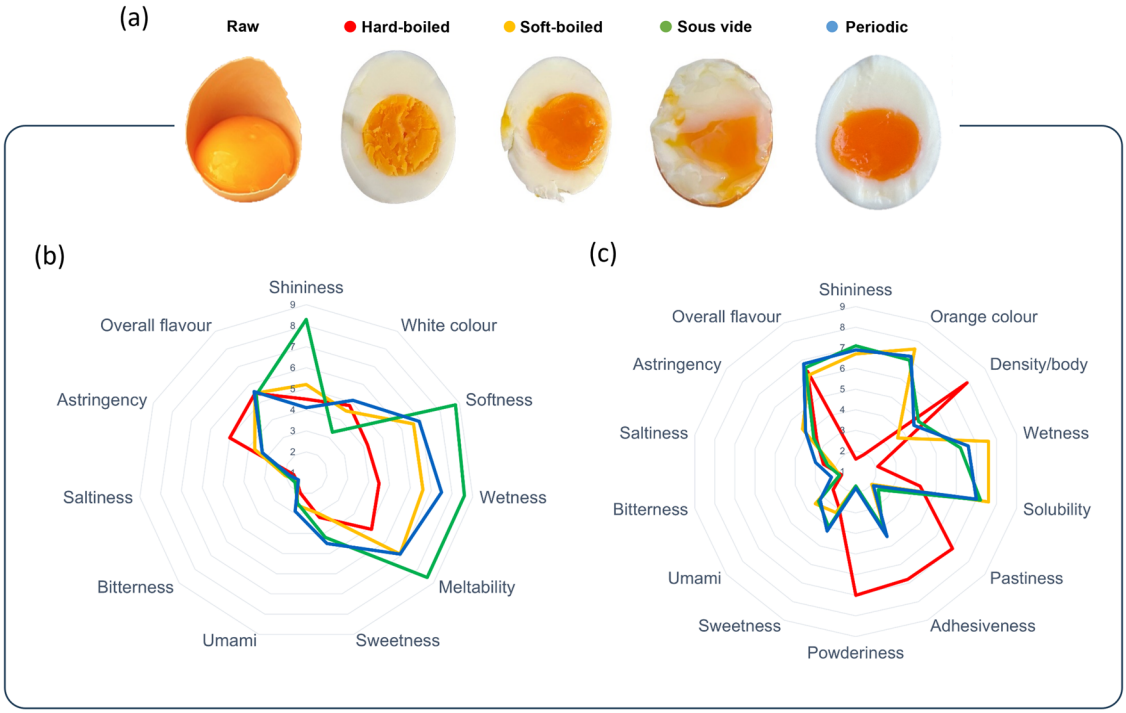

Fig. 1 | Sensory analysis of eggs cooked by different methods. a Eggs were cooked using various cooking techniques. Objective sensory analysis performed on **b** the albumen and **c** yolk. The periodic method led to an albumen similar to soft-boiled, and a yolk similar to sous vide, demonstrating delivery of two different textures and tastes using only one cooking method. (From Fig. 4 of the original publication).

Vision-based tactile sensor design using physically based rendering, Arpit Agarwal et al.

Vision-based tactile sensors (VBTSs) are a key technology for both current and future robots. However, designing compact and high-resolution VBTSs remains a major challenge due to the need for the compact integration of multiple optical components. Changes in the optical system, including illumination patterns, can significantly affect sensing accuracy. Current design processes often rely on labour-intensive, error-prone human expertise and trial-and-error experimentation, largely because accurate simulation tools for the design and optimization of such devices have been unavailable.

A study published in *Communications Engineering* introduced a framework for designing VBTSs using optical simulation to generate tactile images[7]. Physically based rendering simulated light propagation in arbitrary scenes, enabling the exploration of how different design parameters influence performance. A procedural generator produced new sensor designs with controllable shapes, materials and light settings. Alongside the generated tactile images, a design evaluation procedure, RGB2Normal, was used to quantitatively assess sensor design performance. When applied to a curved surface (a robotic fingertip), the framework produced a new sensor design that performed 35% better in 3D surface reconstruction accuracy in simulation compared to the previous state-of-the-art human-expert design, and a 15% improvement on real sensors. In addition, the generated design performed 5 times better than previous state-of-the-art human-expert design in real-world robotic tactile embossed text detection.

Arpit Agarwal and colleagues' framework substantially accelerated the VBTS design process, cutting development time from several months to weeks. The resulting optimised sensor could be installed on various parts of a robot, such as the fingertips, to enhance tactile perception by providing high-resolution contact signals, even when approaching an object from multiple directions to perceive it (Fig. 2). The proposed technology was demonstrated in two robotic tasks: robotic grasping and embossed text detection.

The proposed framework for full sensor design proved effective in automating the design of VBTSs, outperforming human design based on trial-and-error approaches. Unlike existing optical simulation tools, which are limited to flat surfaces, this framework also supports the design of sensors with curved geometries. This feature significantly expands the potential application range of these sensors. *Pedro Neto*

Array of micro-epidermal actuators for noninvasive pediatric flexible conductive hearing aids, Enosh Lim et al.

Permanent conductive hearing loss in children can often be resolved surgically, but the procedures are highly invasive. Non-surgical conductive hearing aids require additional retention devices, which introduce risks of instability and can cause skin reactions. Flexible hearing aids could be an attractive alternative, yet they face the challenge of generating sufficiently strong vibrations under strict constraints on driving voltage, device size, and structure. Increasing the number of transducers to form an array is a feasible way to enhance the vibration of flexible hearing aids, but it requires the vibrational waves produced by individual transducer units to interfere constructively. Now, Lim and colleagues, writing in *Communications Engineering*, report an exploration of how the mechanisms by two transducers in a flexible hearing aid can achieve constructive interference, further boosting the device's vibration level[8].

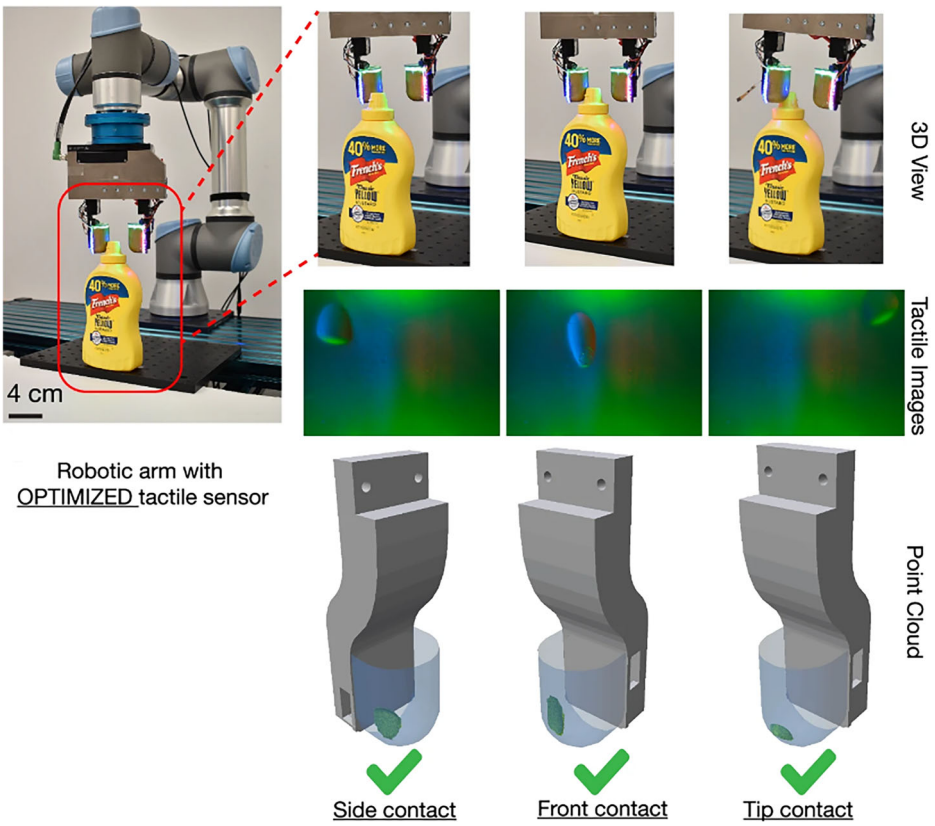

Fig. 2 | The curved vision-based tactile sensor enables object manipulation without the need to reorient the robotic arm. Robot's setup, the tactile images and the 3D surface reconstruction obtained from three different approach directions (side, front and tip). (From Fig. 8 of the original publication).

To maximize vibration output, the researchers designed a micro-epidermal actuator (MEA) array featuring two configurations: horizontal and stacked (Fig. 3). Simulations and experiments showed that the arrays generated constructive interference on bone or the device shell, delivering markedly higher vibration velocity and a wider controllable bandwidth than a single unit, with phase control enabling steerable vibration directivity. In clinical testing, the stacked dual-MEA improved output by about 12.1 dB at 250 Hz and 13.8 dB at 500 Hz versus a single MEA. Relative to the unaided ear, the dual-MEA provided a 30.5 dB improvement at 1 kHz and an average gain of ~20.5 dB across 0.25–8 kHz. The minimum drive voltage required for audibility dropped by ~71% with the array.

This work shows that MEAs on thin, flexible platforms can overcome soft-tissue damping and reduce the drive threshold, charting a practical route to noninvasive, child-friendly conductive hearing assistance. The combination of steerable directivity reduced power needed to reach audibility, and a flattened frequency response speaks directly to real-world usability, comfort, and social acceptance, and lays the groundwork for multicenter trials and integration with low-power electronics. *Liangfei Tian*

Submersible touchless interactivity in conformable textiles enabled by highly selective overbraided magnetoresistive sensors, Pasindu Lugoda et al.

Electronic textiles are establishing themselves as a promising platform for wearable devices, human-machine interfaces, and physiological monitoring systems. However, integrating functional sensors into fabrics without compromising comfort, flexibility, and mechanical strength remains a significant challenge. Tactile or capacitive interaction technologies are more susceptible to suffering from accidental activations, hysteresis, moisture sensitivity, and degradation after repeated deformation or washing. There is still a need to develop sensors with touchless interaction mechanisms that combine selectivity, mechanical robustness, and reliable operation under extreme conditions, including submersion, without compromising textile comfort.

In their contribution, Pasindu Lugoda and colleagues introduced an innovative approach to this problem[9]. They demonstrated a truly conformable integration of flexible magnetoresistive sensors directly into the core of textile braids, creating so-called overbraided magnetoresistive sensors. Exploring a simple nanostructured Cu/Co giant magnetoresistive sensor, thin films deposited on flexible substrates (polyimide film) were encapsulated in mechanically resilient braided yarns, ensuring stable electrical connections and compatibility with conventional textile processes. The resulting sensors maintained sub-μT detection performance, withstood extensive deformation, shear, and machine-washing cycles, and operated reliably underwater (Fig. 4). The authors showed the successful application of the sensors on an interactive sleeve for virtual reality navigation and a helmet strap capable of detecting secure closure.

The demonstration of touchless magnetic interactivity in rugged textiles represents a substantial advance in wearable engineering. Unlike capacitive or tactile sensors, magnetic activation avoids false triggers and remains stable in humid environments, paving the way for critical applications in safety, protective equipment, industrial operations, surgical environments, and underwater activities. Low energy consumption also enables integration with energy harvesting systems, bringing these textiles closer to self-

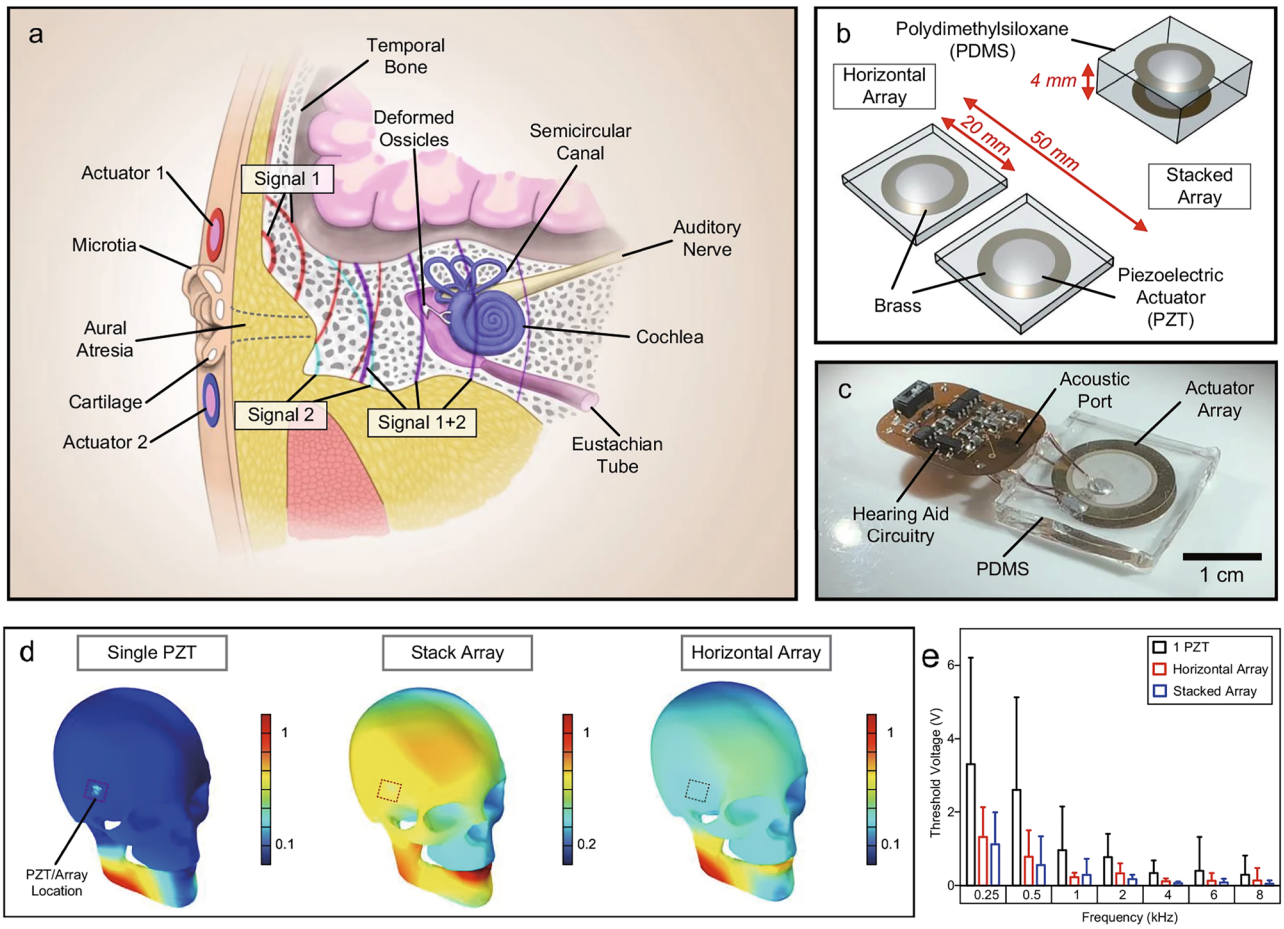

Fig. 3 | Concept of the micro-epidermal actuator array. a Illustration of a horizontal array attached to a patient with aural atresia. Vibrational signals are generated by each actuator, constructively interfering with the bone to produce a stronger signal. The cochlea picks up the combined vibrations and transmits the auditory signal to the brain. **b** Schematic of a horizontal and stacked array in flexible substrates. **c** A single-phase hearing aid device with a stacked array. **d** Comparison of PZT and arrays on a human skull at 600 Hz. Arrays distribute the vibrations across a larger surface area. **e** Minimum voltage required for the MEA/array to produce an audible vibration for the subject. The error bars represent the standard deviation from measuring 10 subjects. (Panels taken from Figs. 1, 2, and 4 of the original paper).

sustaining solutions. The most notable aspect of the work is the sensor's isotropic activation: magnetic fields from any direction generate a consistent response, allowing for natural and intuitive interaction without the need for precise alignment. This characteristic makes the technology exceptionally suitable for everyday textiles, where the orientation between user, fabric, and actuator is rarely controlled. *Cecilia de Carvalho Castro Silva*

Monolithically integrated ultra-wideband photonic receiver on thin film lithium niobate, Marco Moller de Freitas et al.

As the demand for higher data capacity in wireless and mobile communications continues to grow, traditional electronic microwave systems are reaching their limits, especially at millimeter-wave and terahertz frequencies. When operating at these higher frequencies, the performance of electronic devices tends to degrade, restricting their ability to support wider bandwidths and faster data rates. To overcome these limitations, researchers have turned to microwave photonics, which combines optical and electronic technologies to achieve much broader operational bandwidths. However, integrating both electronic and photonic components on a single chip has remained a major technical challenge, mainly due to the high dielectric permittivity of commonly used materials like silicon, indium phosphide, and lithium niobate.

An article by Freitas et al.[10] addressed that challenge by demonstrating a photonic receiver built on thin-film lithium niobate (TFLN) with a quartz handle. The receiver integrated a broadband antenna and a low-drive-voltage electro-optic modulator (Fig. 5), achieving efficient performance at high frequencies. Using this device, the researchers demonstrated a free-space data link capable of transmitting data at rates up to 2.7 gigabits per second and an error vector magnitude as low as 3%. These results highlight the strong potential of TFLN as a material platform for combining radio-frequency and photonic functions within a single, compact device.

The work represents an important step forward in developing high-speed, energy-efficient, and scalable systems that could support the next generation of wireless communication technologies. Beyond the results, the research points to a broader technological impact: it opens a pathway toward practical, ultra-wideband communication systems operating in the millimeter-wave and terahertz range, with

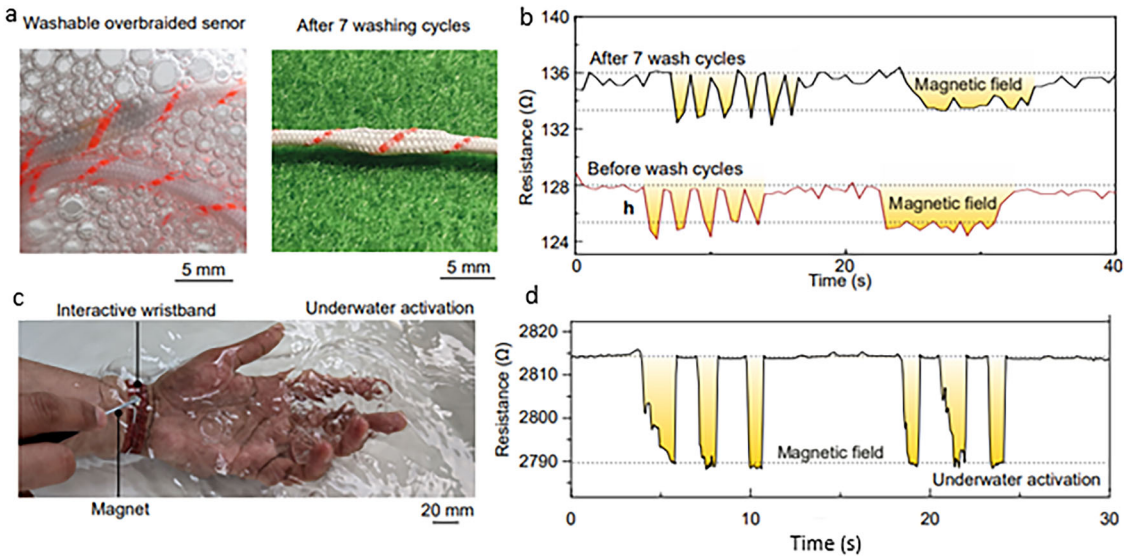

Fig. 4 | Overbraided magnetoresistive sensors operate reliably underwater. **a** Photograph of an overbraided magnetoresistive sensor during washing and after seven wash cycles in a washing machine. **b** Response of the overbraided magnetoresistive sensor to an approaching permanent magnet before and after seven machine wash cycles. **c** Activations of a smart wristband in underwater conditions. **d** The overbraided magnetoresistive sensor is activated reliably in underwater conditions when a permanent magnet is approached. (From Fig. 2 of the original paper).

potential applications in 6 G networks, radar, and advanced sensing systems. *Chaoran Huang*

Colloidal-fibrillar composite gels demonstrate structural reinforcement, secondary fibrillar alignment, and improved vascular healing outcomes, Nina A. Moiseiwitsch et al.

The porosity of biomaterial scaffolds for tissue engineering applications is of critical importance for the promotion of cellular infiltration and healing. Hydrogel scaffolds of precise porosity can be achieved by annealing colloidal nanoparticle building blocks. But these structures lack the fibrillar architecture found in native extracellular matrices which have greater load bearing properties and propensity to natural tissue remodelling. Is it possible to create a tunable hydrogel with controlled porosity and a fibrillar architecture, to achieve the best of both worlds? In a publication in *Communications Engineering*[11], Nina A. Moiseiwitsch and colleagues reported exactly such a material system and investigated its application as a vascular surgical sealant.

Composite gels were formed through the addition of fibrin nanoparticles to whole blood fibrin gels in a variety of compositions which were then put through a raft of mechanical and rheological analyses. Cryogenic scanning electron microscopy of the gels revealed three different structural architectures: a nanoparticle-reinforced fibrillar fibrin composite structure at low nanoparticle concentrations, a dual matrix structure of nanoparticle networks and fibrillar networks at high concentrations, and both fibril reinforcement and an aligned secondary colloidal structure at intermediate concentrations.

The researchers chose a composition at an intermediate concentration of nanoparticles for further examination in vivo to optimise both structural alignment and mechanical properties. Gels were applied as a suture-line surgical sealant to prevent leakage in arterial repair in a rabbit model in vivo. After one week post-op, the nanoparticle composite gel resulted in smaller wounds as a percentage of vessel cross-sectional area than either stitches alone or a commercially available high density fibrin glue. Additionally, the nanoparticle-treated vessels demonstrated greater endothelial continuity than fibrin glue-treated vessels, indicating more effective tissue remodelling. And at three weeks, endothelial hypertrophy was significantly less in composites groups than the fibrin glue group. Transcriptomic analysis suggested less collagen and greater inflammation in the fibrin glue-treated tissue which may account for the differences in outcomes in vivo.

The paper is a great demonstration of careful investigation across compositions being used to reveal a Goldilocks effect, a sweet spot of optimal structure and properties, which can then be harnessed to create exciting translational opportunities. Finally, this paper has 11 women in the author team, which is rare in an engineering contribution and something to be celebrated. *Rosamund Daw*

An integrated wireless system for dynamic strain monitoring of Einel-rad-Einelfahrwerk bogies for high-speed rail transport, FengLong Wang et al.

Railways are advancing toward higher speeds and tighter service intervals, demanding reliable condition monitoring of vehicle bogies that experience complex and fluctuating loads. Fenlong Wang, Yating Yu, Zhiwen Luo, et.al address this challenge through an elegant, fully integrated wireless system designed for real-time dynamic strain monitoring of Einel-rad-Einelfahrwerk bogies used in high-speed rail transport[12]. The developed system combines radio-frequency identification technology, a microcontroller for analogue-to-digital conversion, and strain sensors within a compact monitoring node capable of sampling at 200 Hz (Fig. 6). Data are wirelessly transmitted from the bogie's axle or wheel-hub assembly to a reader located approximately 70 cm away. Laboratory calibration within the 600–1400 με range yielded absolute errors below 19.4 με (≈2.1 %), while field tests on operational trains showed maximum errors of 5.1 με (≈7.5 %) for axle strain and 7.6 με (≈7.7 %) for wheel-hub lateral strain.

This advancement has major implications for structural health monitoring in railway engineering. Compared with conventional wired or

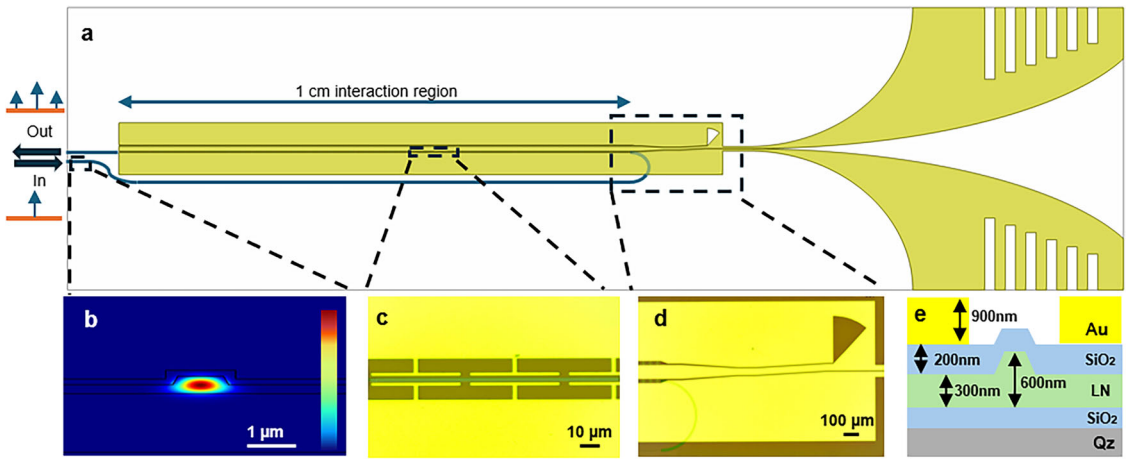

Fig. 5 | Ultra-wideband antenna coupled photonic receiver on thin-film lithium niobate (TFLN). a Scaled image of the whole device showing the antenna coupled to the folded phase modulator with input and output optical waveguides at the left edge. **b** Simulated optical mode within the ridge-etched TFLN waveguide. **c** Microscope image of the fabricated device showing the segmented electrodes and the ridge-etched waveguide in the 5-μm gap between the T's. **d** Microscope image of the balun with the stub, the signal-electrode-width transition and the transition for the segmented electrodes. **e** Cross-section view of the device with quartz (Qz), silicon dioxide (SiO_2), lithium niobate (LN), and gold (Au). (From Fig. 1 of the original publication).

Fig. 6 | RFID dynamic strain monitoring system block diagram (from Fig. 3 of the original publication).

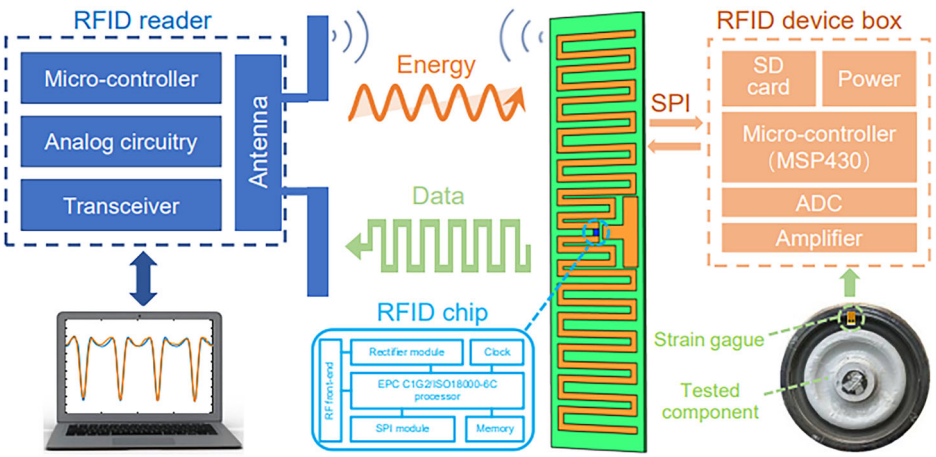

periodic inspection methods[13], the proposed system allows continuous, high-sampling-rate strain monitoring in harsh electromagnetic and vibration-rich environments. Such capability enables real-time condition assessment and predictive maintenance - key steps toward safer and more efficient railway operations. Specifically, the analog-to-digital conversion design effectively mitigates environmental electromagnetic interference. Furthermore, its low-cost and modular architecture could be adapted for other rolling-stock components and even for broader rail infrastructure applications. What stands out most is the authors' clever balance between high-speed data acquisition and wireless transmission reliability, a long-standing challenge in metallic, vibration-intensive environments. The demonstrated performance under real-world loading confirms the system's potential for direct field deployment rather than remaining a laboratory prototype. Looking ahead, the system demonstrates strong potential for integration with AI algorithms and IoT platforms to enable advanced predictive maintenance and early anomaly detection. *Said Elias*

Industrial-scale prediction of cement clinker phases using machine learning, Sheikh Junaid Fayaz et al.

The process of manufacturing cement is extremely energy-intensive and contributes nearly 7% of global CO_2 emissions[14]. The mineralogical phases of clinker (i.e., alite, belite, aluminate, and ferrite) dictate the performance, durability, and sustainability of cement[15]. However, traditional Bogue equations and physics-based models are inaccurate or too complex for predicting these phases in full-scale operations, as they cannot capture the nonlinear and time-varying nature of kiln processes[15]. This limitation has long hindered real-time quality control and optimization in cement manufacturing.

Sheikh Junaid Fayaz and colleagues developed a machine-learning (ML) framework trained on a two-year industrial dataset comprising 8,654 clinker compositions from an operating cement plant[15]. Among nine benchmarked ML architectures, the best performing

model for alite was neural network with 1.24% mean absolute percentage error (MAPE), for belite was Gaussian process regression with 6.77% MAPE, and for ferrite was support vector regression with 2.53% MAPE; this demonstrated an 88% improvement over traditional Bogue calculations. The models proved robust under fluctuating industrial conditions and were interpreted using explainable-ML methods. Through SHapley Additive exPlanations (SHAP) analysis, the authors revealed the hierarchical and directional influence of clinker oxides on phase formation: CaO strongly promoted alite formation, while SiO_2 exhibited a negative correlation—findings that align with classical clinker chemistry and lend credibility to the model's interpretability.

The framework enables proactive, real-time prediction of clinker phases, allowing plant operators to optimize kiln temperature and fuel input before production deviations occur. This predictive control reduces over-burning, fuel waste, and CO_2 emissions while maintaining product quality[15]. Moreover, by forming the computational foundation for "digital twin" models, the approach allows continuous monitoring and early detection of off-specification clinker, representing a transformative step toward data-driven, low-carbon cement manufacturing.

What makes this contribution particularly notable is the combination of industrial realism and interpretability. Unlike prior laboratory or simulation-based studies, this work validates explainable ML using large-scale plant data. The SHAP visualization effectively bridges data science and materials chemistry, transforming a black-box prediction model into a transparent decision-support tool for sustainable process control. *Ali Behnood*

Powered knee exoskeleton improves sit-to-stand transitions in stroke patients using electromyographic control, Andrew J. Gunnell et al.

For many individuals after stroke, regaining the foundational movements required for activities of daily living (and ultimately for functional independence) is a core goal of rehabilitation. Sit-to-stand transitions are particularly important as they precede numerous daily tasks and demand coordinated lower-limb control, strength and balance that can be compromised after stroke. Mechatronic assistive devices that augment lower limb function hold promise in addressing this challenge, yet many depend on preprogrammed trajectories or manually tuned torque profiles, which can limit the user's ability to adapt assistance to their capabilities and engage in natural movement patterns.

In the paper *"Powered knee exoskeleton improves sit-to-stand transitions in stroke patients using electromyographic control,"*[16] Andrew J. Gunnell and colleagues demonstrate an alternative control approach for a powered knee exoskeleton that derives control signals directly from electromyographic (EMG) measures of muscle activation in the limb. By leveraging these neuromuscular signals, the exoskeleton can adapt its assistance in real time, responding dynamically to the user's intent rather than imposing predetermined movement trajectories or torque profiles.

The findings show that stroke survivors using the EMG-controlled exoskeleton exhibited improved sit-to-stand performance across multiple metrics including time to stand, weight-bearing symmetry, and peak quadriceps activation and knee torque on the affected side. Notably, the EMG-based control approach also shifted several of these measures closer to those observed in an able-bodied control cohort. These results demonstrate that biomechanical improvements can be achieved without extensive calibration or reliance on predetermined movement trajectories, and that some individuals with limited or impaired voluntary muscle activity can effectively engage with EMG-driven robotic assistance.

This work stands out in integrating the motor capabilities of stroke survivors with the technological capabilities of powered knee exoskeletons. Specifically, the results suggest that in some cases muscular signals that are often quite variable in stroke survivors may still be leveraged to produce adaptive and more physiologically appropriate assistance during sit-to-stand transitions. These findings have important implications for assistive systems in stroke rehabilitation and broader efforts to develop patient-specific, adaptive mechatronic devices, supporting EMG-based (or neuromotor-derived) control as a promising approach for enabling more personalized and responsive neuro-robotic interventions. *Jonathon Schofield*

Scalable reinforcement learning for large-scale coordination of electric vehicles using graph neural networks, Stavros Orfanoudakis et al.

The accelerating transition to electric mobility presents one of the greatest challenges for modern power systems. As the number of electric vehicles (EVs) grows, so too does the complexity of managing their charging in real time, ensuring grid stability while meeting user expectations. Traditional optimisation approaches—while effective at small scales—struggle to cope with the high dimensionality and dynamism of large EV networks.

Orfanoudakis and colleagues[17] introduce a scalable reinforcement learning framework that addresses this challenge head-on. Their model, termed EV-GNN, combines reinforcement learning with graph neural networks to coordinate the charging behaviour of thousands of vehicles simultaneously. By representing the charging infrastructure as a graph—linking vehicles, chargers, and transformers—the system captures the physical and operational relationships among network components. This structure allows the algorithm to focus only on relevant actions, improving both learning efficiency and real-time decision-making.

Tested on simulations of networks with up to a thousand charging points, EV-GNN outperformed conventional reinforcement learning baselines across multiple criteria, including energy-tracking accuracy, user satisfaction, and scalability. Importantly, the model also demonstrated strong generalisation when transferred to new environments, hinting at practical potential for deployment in real-world charging operations.

The impact of this work extends beyond EV management. It exemplifies how domain-aware machine learning architectures—in this case, a graph representation of an engineered system—can overcome the scalability limits of generic AI approaches. As energy systems become more distributed and data-rich, such intelligent coordination frameworks may underpin the next generation of smart-grid control.

What stands out most in this paper is its union of elegance and utility: a clear demonstration that embedding system structure within learning algorithms can turn a long-standing scalability bottleneck into a tractable, efficient solution. It marks an exciting step toward the self-optimising energy networks of the electrified future. *Alessandro Rizzo*

Scorecard for synthetic medical data evaluation, Ghada Zamzmi et al.

In addition to advanced hardware resources, efficient optimization, and new computational architectures, a key driver in the dramatic development of deep learning algorithms and their substantial impact is the availability of big data. While large datasets of handwritten digits and labeled natural images can be relatively easily extracted from the web[18], medical data is scarcely made publicly available due to subject confidentiality, hospital regulations, the high cost of expert annotators, and profit considerations. This challenge is further exacerbated for rare diseases and underrepresented minorities.

In recent years, considerable attention has been brought to AI architectures that can

synthesize highly realistic data (with the prominent examples including variational autoencoders, generative adversarial networks, and diffusion models), suggesting a means to circumvent the need for large medical datasets. However, the lack of a framework for evaluating the quality and appropriateness of this data under meaningful medical contexts may result in poor network training, unrealistic features and hallucinations, and hinder the effectiveness of synthetically augmented medical AI.

This year, Zamzmi et al. from the U.S. Food and Drug Administration described a novel transparent and comprehensive framework for synthetic medical data evaluation[19]. They introduced a quantitative assessment based on seven Cs: Congruence, Coverage, Constraint, Completeness, Compliance, Comprehension, and Consistency. Each of these criteria was embedded within a practical scorecard, providing a multimodal assessment of the synthetic medical data, including alignment with patient data, representation of unique samples, plausibility in relation to real data, and adherence to physical/biological constraints.

Importantly, the authors detailed quantitative metrics specifically relevant for medical images and large language models, highlighting the weaknesses of existing alternative general metrics when naively applied to medical data (e.g., a statistical fidelity metric used in computer vision would be insufficient to represent holistic medical data).

Using poor-quality or inappropriate synthetic data can substantially affect the AI framework's performance. It is therefore expected that the suggested approach and scorecard will become a valuable tool for various stakeholders in the broader field of medical informatics. *Or Perlman*

3D vector field-guided toolpathing for 3D bioprinting, Meghan Rochelle Griffin et al.

In biological tissues, function is intertwined (or interwoven) with form. This includes not only geometric features of the tissue, but also the complex, fibrous microarchitectures found within these tissues. In organs like the heart these are not random. Their specific alignment and orientation are critical for biomechanical properties and physiological function. While 3D printers have recently been used to provide spatial control of fiber alignment via toolpath deposition, most printers operate by stacking a series of 2D planes, limiting fiber orientation to a set of stacked monolayers. This misses many of the key features of the intricate, non-planar fiber alignments found in biological materials.

A new study by Meghan Rochelle Griffin and colleagues[20] bridges this gap with a novel algorithmic framework called NAATIV3 (Non-planar, Architecture-Aligned Toolpathing for In Vitro 3D bioprinting). The researchers' framework uses data from diffusion tensor magnetic resonance imaging (DTMRI) to translate 3D maps of fiber orientation into a 3D toolpath sequence to produce 3D-printed structures with the same essential features. The authors then applied their workflow to 3D print a model of a human left ventricle.

This work represents a significant leap in toolpath planning for 3D printers by automating the conversion of 3D fields of fiber orientation directly into machine-readable G-code. By solving the challenge of mapping, reducing, and sequencing these fiber orientations into a toolpath sequence, the team has enabled the fabrication of constructs that are structurally faithful to their biological counterparts. NAATIV3 has the potential to be extended beyond cardiac tissue engineering. By enabling the creation of tissue models that accurately reflect specific developmental states, diseases, or patient-specific anatomies, the technology could enable new capabilities in pathophysiological studies more broadly.

NAATIV3's ability to handle general vector fields suggests exciting applications in other industries where fiber alignment are paramount, such as the bioengineering of plant-based materials, bioengineering food, maximizing 3D-fabricated component strength, brain mapping and more. This direct translation of a 3D vector field into a continuous manufacturing process is a unique and versatile approach, offering a new level of fidelity in the pursuit of truly biomimetic materials. *Jordan Raney*

Freeze–thaw recycling for fiber–resin separation in retired wind blades, Khalil Ahmed et al.

Wind energy's rapid expansion is producing a rising wave of end-of-life blades made from glass fibre-epoxy composites that are difficult to recycle. Conventional thermal and chemical routes can separate fibre and resin, but they demand high temperatures, aggressive reagents, and substantial post-treatment tensions that limit circularity and eco sustainability at scale.

Khalil Ahmed and colleagues[21] report a simple eco-friendly alternative: freeze-thaw recycling that uses only water at human-safe temperatures to infiltrate pre-existing microcracks and voids in aged blades. Ice expansion then propagates these defects and selectively debonds the fibre-resin interface. Multimodal characterization (scanning electron microscope, micro- computed tomography (CT), weight change) verifies targeted interfacial degradation without altering epoxy chemistry. Quantitatively, micro-CT reveals ~65% higher crack-volume fraction and ~32% higher connected porosity after ten days of cycling. Meanwhile, nanoindentation shows up to 96% retention of the glass-fibre elastic modulus. This is evidence that the approach weakens the interface yet largely preserves fibre performance. Notably, effluent water remained near-neutral (pH ≈ 6.4) with low total organic carbon (~ 1.3 mg L^{-1}), within World Health Organisation/Environmental Health Agency limits; microplastic fragments were micrometre-scale and readily removed by filtration.

By attacking the interface (not the bulk polymer), freeze-thaw complements mechanical size-reduction and could serve as a low-energy pre-processing step in multi-phase recycling lines. This enables subsequent recovery and reuse of fibres in automotive parts, building materials, and panel boards. The reliance on commodity freezers and reusable water points to favourable techno-economics and easier deployment at decommissioning yards, while reducing environmental burdens typical of thermo-chemical routes. Life-cycle assessment at scale is an important next step.

Two elements are especially compelling: (i) the reframing of "damage" as an asset—repurposing fatigue-induced micro-cracks in service-aged blades to initiate controlled separation—and (ii) the inclusion of a pragmatic environmental check on process water quality alongside materials analytics. Together, they advance a practical, interface-first mindset for retired blade recycling. *Wan-Ting (Grace) Chen*

Real-time monitoring of water states in large-diameter aqueducts—learning from distributed acoustic sensing signals, Dao-Yuan Tan et al.

Large-diameter gravity aqueducts are the unseen backbone infrastructure of urban and regional water supply systems. Detecting unsteady flow conditions that trigger critical events (such as air pocket effects and water hammer) is essential for ensuring stable hydraulic operation and protecting structural integrity. However, monitoring these complex and transient flows remains challenging. Conventional tools such as closed-circuit television (CCTV), ultrasonic sensing and microwave tomography provide point-based inspection of flow patterns and transitions inside deeply buried pipelines[22]. However, these monitoring techniques leave utilities with limited capability for continuous monitoring across pipeline networks. Distributed acoustic sensing

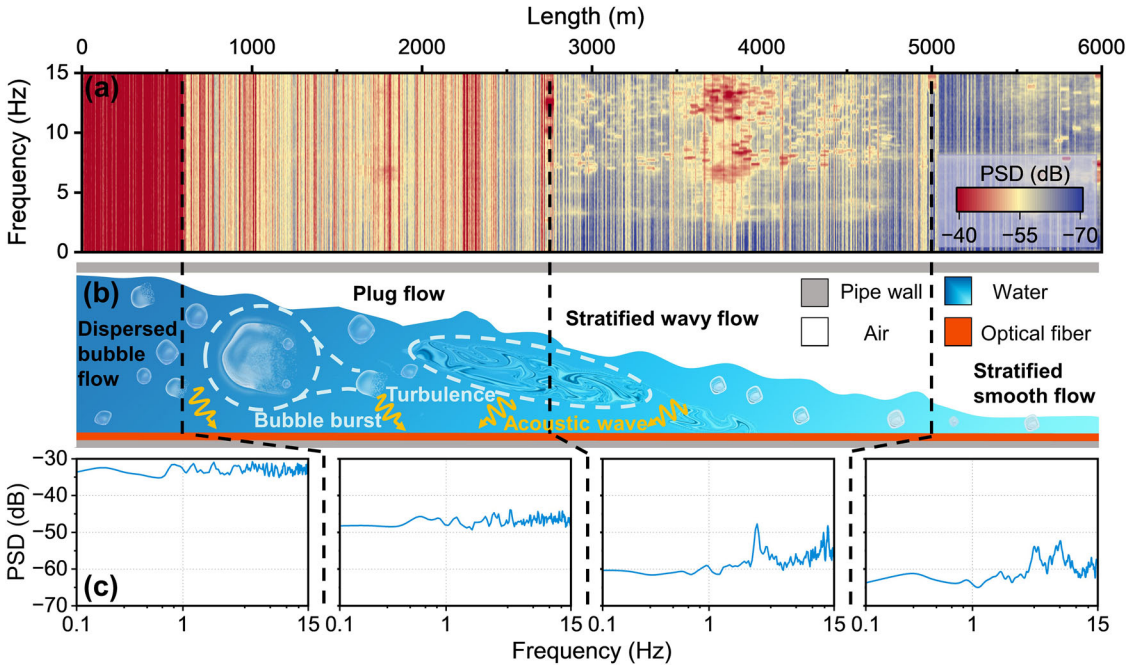

Fig. 7 | Acoustic characteristics during the aqueduct water filling process. a Power spectral density patterns during the aqueduct water filling process, **b** Schematic diagram of the aqueduct water filling process, **c** Power spectral density curve diagrams of the four states of the water filling process. (From Fig. 4 of the original publication).

(DAS), by contrast, can offer real-time monitoring of water status over kilometre-scale distances[23], yet it typically generates spectral data that are challenging to interpret in operational settings.

In their contribution to *Communications Engineering*[24], Dao-Yuan Tan and colleagues introduced a real-time monitoring framework (called DAS-Hydro HierarchyNet) that integrated DAS measurements with a hierarchical deep-learning architecture to classify flow regimes and track water migration along large-diameter aqueducts. Using low-frequency acoustic signatures transformed via power spectral density analysis, the model first detected the presence of water (for example, 6–8 Hz band associated with turbulent acoustic signal) and then discriminated five different flow patterns, including dispersed bubble flow, plug flow, stratified smooth and wavy flow, and dry (empty-pipe) conditions, based on their spectral characteristics (Fig. 7). Applied to 6 km deep-buried section (40–60 m in depth, 2.9 m in diameter) of the Pearl River Delta Water Resources Allocation Project, DAS-Hydro HierarchyNet accurately estimated water location and velocity, and captured the spatiotemporal flow profile during aqueduct filling process, even under low signal-to-noise conditions.

A SHAP-based interpretability analysis further linked specific frequency bands to distinct flow regimes, mitigating black-box behaviour in the model's decision process. This could allow engineers to infer flow states directly from spectral fingerprints when visual inspection is impossible. This technology also supports safer commissioning and operation by complementing conventional point inspections. Taken together, this work demonstrates a scalable and continuous surveillance approach for large-scale subterranean aqueducts, enabling early warning of unexpected hydraulic behaviour indicative of delays, blockages, or other anomalies and contributing intelligent management of critical water infrastructure. *Manabu Fujii*

Optimising housing typology distributions for multi-hazard loss reductions in resource-constrained settings, Arvin Hadlos et al.

Communities worldwide are exposed to multi-hazards—where two or more natural hazards, e.g. earthquakes, or weather events such as typhoons and hurricanes, can occur in the same community[25]. These hazards can have different impacts, i.e. damage rates, on building stocks, meaning there might need to be trade-offs in construction practices to mitigate the impacts from multi-hazards[26]. These trade-offs are important to understand as otherwise whilst a community could be resilient to one natural hazard, a different natural hazard could mean very high damage rates to the building stock, resulting in significant disaster losses. For example, whilst heavy weight, concrete or masonry buildings might perform well under high winds, they can sustain high damage rates during earthquakes.

Arvin Hadlos and colleagues developed an approach to simulate the impact on building stocks of two, independently occurring, natural hazards[27]. This approach was applied in Itbayat, Batanes, Philippines, which is subject to both earthquakes and typhoons. The study showed that a distribution of housing typologies - across a combination of lightweight construction and reinforced concrete, results in lower multi-hazard losses. The researchers also highlighted the importance of socio-technical considerations, such as households' risk perceptions when making any changes to housing stock distribution. This work instils a new way in understanding the vulnerabilities of different communities to multiple natural hazards, with the potential to shape future construction practices to reduce these risks and vulnerabilities. *Danielle Densley Tingley*

StarWhisper telescope: an AI framework for automating end-to-end astronomical observations, Cunshi Wang et al.

The rapid development of large-scale telescope arrays has influenced time-domain astronomy,

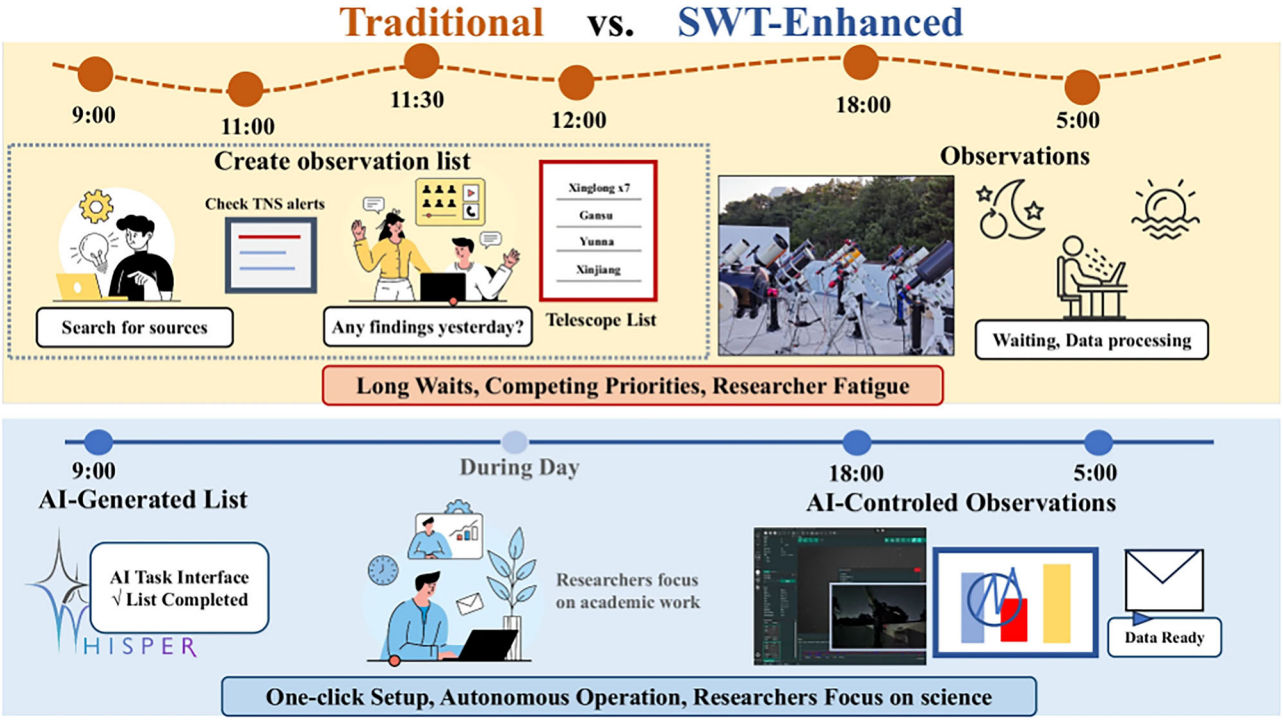

Fig. 8 | Workflow comparison between traditional observation methods and the SWT enhanced system (from Fig. 1 of the original publication).

but their potential is often limited by the substantial labor required for night's observations, execution, and data reduction. Cunshi Wang and colleagues report StarWhisper Telescope (SWT) system, aiming to address this problem by introducing an AI-driven framework that automates end-to-end astronomical observations across networks of amateur telescopes[28] (Fig. 8). Situated within the context of large upcoming facilities like the Global Open Transient Telescope Array (GOTTA), the SWT framework responds to a critical operational bottleneck, the escalating human cost of running large-scale time-domain surveys.

The paper presents a modular, LLM-based agent system capable of generating observation plans, controlling telescopes through Nighttime Imaging 'N' Astronomy (N.I.N.A.) software integrations, processing data in real time, and issuing automated follow-up recommendations when transients are detected. By deploying SWT on the Nearby Galaxy Supernovae Survey (NGSS), a network of ten amateur-level telescopes, the authors demonstrate the system's capacity to reduce planning time from about 1.5 hour per telescope to under a minute, while achieving better sky coverage and zero conflicts. Additionally, the system detected multiple transients, including a flare star AT2025pk, with response times comparable to professional surveys.

SWT outlines a blueprint for a future "AI astronomer," wherein autonomous agents make real-time decisions and coordinate follow-up observations. The authors also acknowledge current limitations, including hardware limitations and network-dependent tool-call failures, offering a compelling roadmap toward fully autonomous observatories. *Wenjie Wang*

Enabling multirotor UAVs to perch, land and detach with standard propeller guards, Yuying Zou et al.

Uncrewed aerial vehicle (UAV) "perching" on objects or surfaces is often realised through the addition of specific components, such as claw-like grippers, adhesives, suction cups and magnets. Additions like these, however, can add extra weight, wear out over time, or potentially block onboard sensors or cameras.

Yuying Zou and colleagues suggest a method that involves no extra components: using the multirotor UAV's existing propeller guards themselves[29]. For flat, non-horizontal surfaces, a UAV can activate its propellers, where the "ceiling effect" (an aerodynamic phenomenon that produces a low-pressure area between the surface and propeller) draws the rotors towards the surface, enabling power savings of 1.8–3 times compared to simply hovering mid-air (Fig. 9). For rougher surfaces, increased friction between the surface and propeller guards further reduces the necessary propeller thrust. The researchers demonstrated the landing, perching and detaching operation in a range of surface orientations (0°, 45°, 90°, 135°, and 180°), with varying surface materials, in the presence of wind, and in real-world outdoor locations.

This paper caught my eye due to its simplicity: why add more components when the existing rotors can do the job? The researchers discuss some potential limitations. Power is required to maintain a perching position, where attachments like grippers would negate the need for any power usage. A flat surface at least the size of the UAV is required, and the propeller guards can wear down over time from physical contact with that surface. However, removal of additional perching components enabled a unique benefit. UAV cameras and sensors are often placed on the underside, the same side where grippers or other attachments are placed. This leads to a partially obstructed field-of-view for those sensors during flight and a significantly or completely obstructed view during perching. Removing these attachments enabled a full unobstructed 360° range for sensors and cameras during flight and during perching, as the topside of the UAV can be used for perching. This allows sensor use during

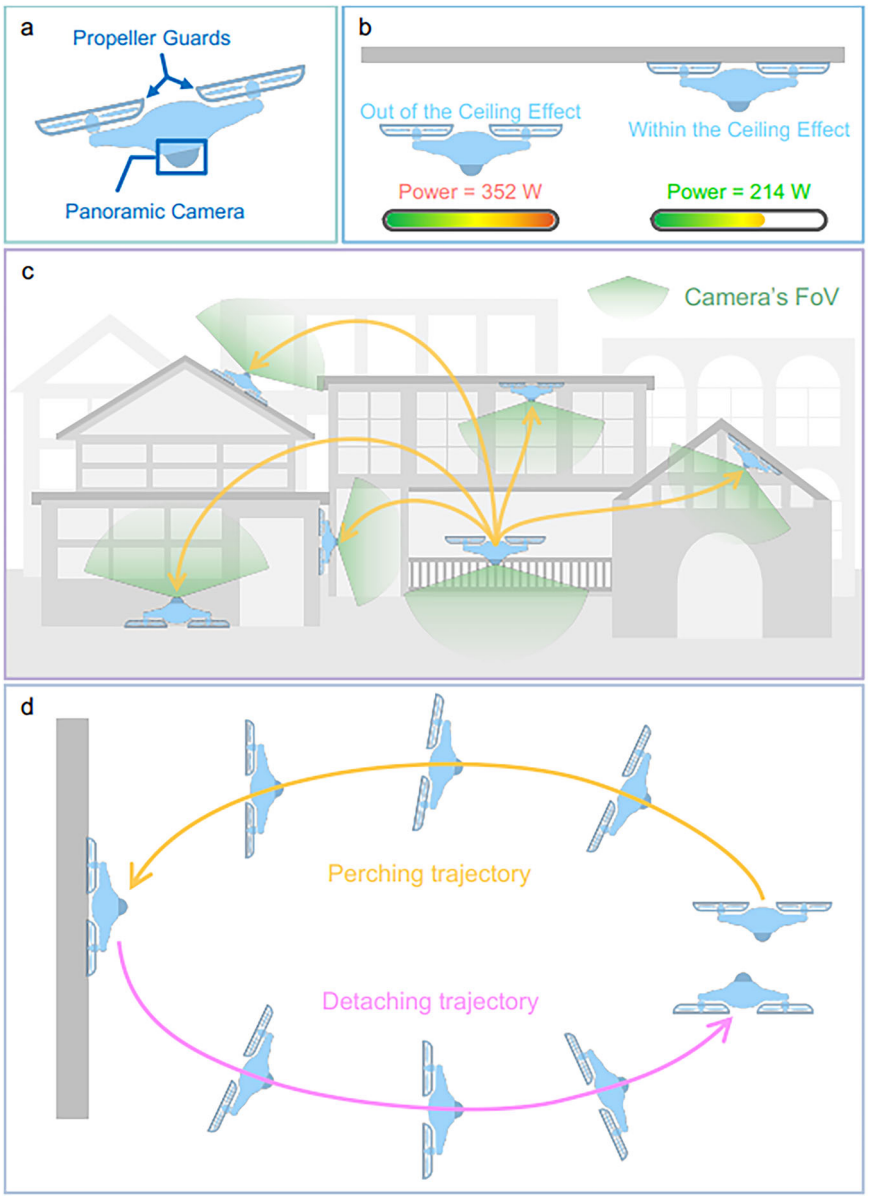

Fig. 9 | A multirotor UAV that perches, detaches, and lands all with its propeller guards. a A conceptual multirotor equipped with a panoramic camera at the bottom. **b** The power reduction due to the ceiling effect, which arises when the multirotor perches on a surface (e.g., ceiling) with its propeller guards. **c** The multirotor is perched on different surfaces, including the ceiling, wall, slope, and ground. **d** The multirotor is perched on and detaching from a wall. (From Fig. 1 of the original publication).

more UAV operational modes, improving overall task efficiency. *Philip Coatsworth*

Pillar arrays as tunable interfacial barriers for microphysiological systems, Ishan Goswami et al.

Microphysiological systems and organ-on-chip (OoC) technology are revolutionizing drug discovery and disease modeling. They have emerged as powerful in vitro platforms that recapitulate key physiological cues for the culture of microtissues, spheroids, and organoids by providing relevant synthetic microenvironments. Most OoC devices exploit microfluidics and geometrical compartmentalization that capture native tissue architecture in a tissue chamber and media channels that provide dynamic delivery of nutrients[30]. The interfaces between compartments play a critical role in maintaining functional separation and enabling chemical communication via the exchange of biomolecules and nutrients. A variety of methods including phaseguides, wetting contrasts, and porous membranes have been conveniently employed to generate interfacial barriers[31]. However, the need for an all-purpose, highly controllable interfacial barrier has long been the field's holy grail. In this work, Ishan Goswami, Kevin E. Healy, and colleagues[32] demonstrate that arrays of micropillars can be designed to achieve interfacial barriers with a high degree of control over rate of diffusion (permeability) and burst pressure. The researchers demonstrate how geometric parameters control the diffusion rate and the burst pressure via fluid dynamics simulations and experiments. The fabrication process involves sophisticated multiple steps of photolithography to produce a master used for subsequent replica molding. At the cost of such intricate processing, the method is conducive to producing highly tunable barriers which support generation of robust tissues via the control over burst pressure and physiologically-relevant nutrient diffusion between the cell and the media compartments. The researchers demonstrate efficacy of their

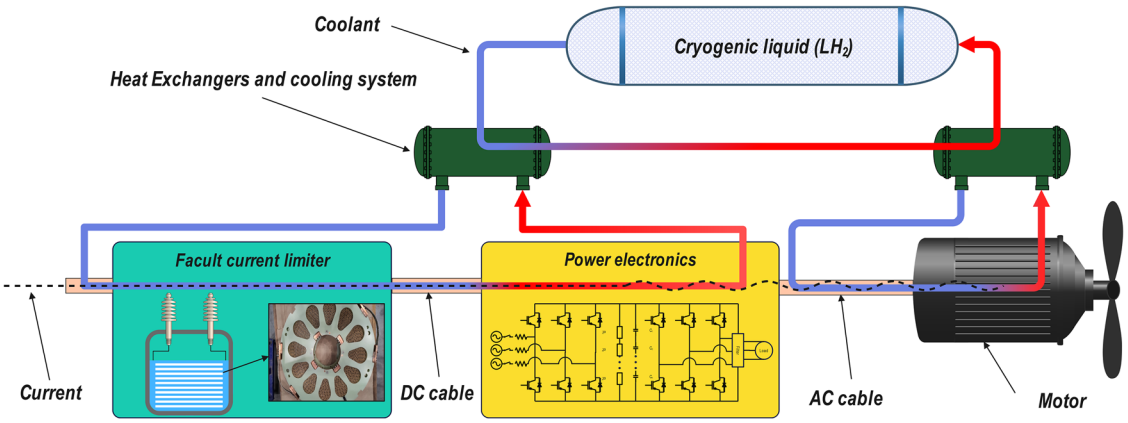

Fig. 10 | An illustration of a cryo-electric propulsion system (from Fig. 1 of the original publication).

approach in a two-compartment OoC device for 3D cardiac and islet microtissues and in a heterotypic model of cardiac tissue and endothelial cells. Their interfacial barrier design allows easy scaling for multi-organ systems and expands the toolkit available to OoC device designers to control the topography of OoC microenvironments. *Massimo Mastrangeli*

Advanced deep-learning model for temporal-dependent prediction of dynamic behavior of AC losses in superconducting propulsion motors for hydrogen-powered cryo-electric aircraft, Shahin Alipour Bonab et al.

The aviation industry is proactively seeking ways to reduce emissions by transitioning to cleaner and more sustainable air travel and is exploring means to achieve net-zero emission commercial aviation; a good example is the Airbus ZEROe project. The concept of hydrogen-powered cryo-electric aircraft, which integrates liquid hydrogen (LH_2) as fuel and the coolant for superconducting components, is emerging as a promising solution (Fig. 10). Industrial demonstrator projects like Airbus UpNext's ASCEND and Cryoprop are pioneering these efforts, picturing future aircraft propulsion systems that utilize the benefits of superconducting technology to dramatically improve efficiency, increase specific power density, and reduce aviation's carbon footprint. However, even small losses at cryogenic temperatures translate into major cooling penalties, extra weight, and system-level design compromises. Accurately predicting these losses and their time-dependent behavior has remained a bottleneck from both design and operation viewpoints.

In a contribution in *Communications Engineering*, Researchers from University of Glasgow in collaboration with engineers from Airbus SAS and Airbus UpNext, solve this problem by developing deep learning surrogate models for both average and time-dependent dynamic AC loss prediction in superconducting propulsion motors[33]. Using a large dataset generated from high-fidelity finite element analysis (FEA) simulations, the authors benchmarked 14 different AI and non-AI techniques. The standout performer was a cascade-forward neural network (CFNN), which achieved near-perfect accuracy for average losses (R-squared is 99.994%) and learned the full time-dependent morphology of AC loss waveforms with equal precision. Once trained, the dynamic model predicted losses in under 9 ms, and this can further be decreased by using near-real-time fast-computation techniques.

The impact of this work lies in it effectively solving one computational bottleneck in cryo-electric aircraft design by AC loss modeling. Designers can now run large parametric studies, explore transient operating conditions, and integrate superconducting motors into full powertrain simulations without the need for slow electromagnetic FEA solvers. In addition, it can be used for the motor configurations that are out of the training range in the initial dataset. Overall, this work shows that AI-based surrogate models have great potential for enabling high-accuracy, low-latency loss predictions to achieve optimal performance superconducting propulsion motor (and other superconducting powertrain devices) in aircraft powertrain design. *Wenjie Wang*

Pengfei Liu[1], Philip Coatsworth[2], Pedro Neto[3], Liangfei Tian[4], Cecilia de Carvalho Castro e Silva[5], Chaoran Huang[6], Rosamund Daw[2] ✉, Said Elias[7], Ali Behnood[8], Jonathon S. Schofield[9], Alessandro Rizzo[10], Or Perlman[11], Jordan Raney[12], Wan-Ting Grace Chen[13], Manabu Fujii[14], Danielle Densley Tingley[15], Wenjie Wang[16] & Massimo Mastrangeli[17]

[1]School of Naval Architecture, Ocean, Energy and Power Engineering, Wuhan University of Technology, Wuhan, China. [2]Communications Engineering, Springer Nature, London, UK. [3]University of Coimbra, CEMMPRE, Department of Mechanical Engineering, Coimbra, Portugal. [4]Department of Biomedical Engineering, Zhejiang University, Hangzhou, China. [5]Mackenzie Presbyterian University, MackGraphe—Mackenzie Institute for Research in Graphene and Nanotechnologies, São Paulo, Brazil. [6]Department of Electronic Engineering, the Chinese University of Hong Kong, Hong Kong SAR, China. [7]Institute for Risk and Reliability, Leibniz University Hannover, Hannover, Germany. [8]Department of Civil Engineering, University of Mississippi, University, Oxford, MS, USA. [9]Mechanical and Aerospace Engineering, University of California Davis, Davis, CA, USA. [10]Dipartimento di Elettronica e Telecomunicazioni, Politecnico di Torino, Torino, Italy. [11]School of Biomedical Engineering and Sagol School of Neuroscience, Tel Aviv University, Tel Aviv, Israel. [12]Department of Mechanical Engineering & Applied Mechanics, University of Pennsylvania, Philadelphia, PA, USA. [13]Department of Plastics Engineering, University of Massachusetts Lowell, Lowell, MA, USA. [14]Department of Civil and Environmental Engineering, School of Environment and Society, Institute of Science Tokyo, Tokyo, Japan. [15]School of Mechanical, Aerospace, and Civil Engineering, University of Sheffield, Sheffield, UK. [16]Communications Engineering, Springer Nature, Beijing, China. [17]Department of Microelectronics, Delft

University of Technology, Delft, the Netherlands.
✉e-mail: r.daw@nature.com

Published online: 11 February 2026

References

1. Zhao, L. et al. Intelligent shipping: integrating autonomous maneuvering and maritime knowledge in the Singapore-Rotterdam Corridor. *Commun. Eng.* **4**, 11 (2025).
2. Di Lorenzo, E. et al. Periodic cooking of eggs. *Commun. Eng.* **4**, 5 (2025).
3. Robles-Gil, A. How to make the perfect boiled egg—if you have the patience. *Science* https://doi.org/10.1126/science.zsxifxa (2025).
4. Fox-Skelly, J. The perfect, but slow, way to boil an egg - according to science. *BBC* (2025).
5. Geddes, L. Scientists crack what they say is the perfect way to boil an egg. *The Guardian* (2025).
6. Trofa, M., Di Maio, E. & Maffettone, P. L. Multi-graded foams upon time-dependent exposition to blowing agent. *Chem. Eng. J.* **362**, 812–817 (2019).
7. Agarwal, A. et al. Vision-based tactile sensor design using physically based rendering. *Commun. Eng.* **4**, 21 (2025).
8. Lim, E., Redleaf, M. & Moghimi, M. J. Array of micro-epidermal actuators for noninvasive pediatric flexible conductive hearing aids. *Commun. Eng.* **4**, 28 (2025).
9. Lugoda, P. et al. Submersible touchless interactivity in conformable textiles enabled by highly selective overbraided magnetoresistive sensors. *Commun. Eng.* **4**, 33 (2025).
10. Moller de Freitas, M. et al. Monolithically integrated ultra-wideband photonic receiver on thin film lithium niobate. *Commun. Eng.* **4**, 55 (2025).
11. Moiseiwitsch, N. A. et al. Colloidal-fibrillar composite gels demonstrate structural reinforcement, secondary fibrillar alignment, and improved vascular healing outcomes. *Commun. Eng.* **4**, 67 (2025).
12. Wang, F. et al. An integrated wireless system for dynamic strain monitoring of Einel-rad-Einelfahrwerk bogies for high-speed rail transport. *Commun. Eng.* **4**, 87 (2025).
13. Farrar, C. R. & Worden, K. An introduction to structural health monitoring. *Philos. Trans. R. Soc. A* **365**, 303–315 (2007).
14. Panesar, D. K., Kanraj, D. & Abualrous, Y. Effect of transportation of fly ash: life cycle assessment and life cycle cost analysis of concrete. *Cem. Concr. Compos.* **99**, 214–224 (2019).
15. Fayaz, S. J. et al. Industrial-scale prediction of cement clinker phases using machine learning. *Commun. Eng.* **4**, 94 (2025).
16. Gunnell, A. J. et al. Powered knee exoskeleton improves sit-to-stand transitions in stroke patients using electromyographic control. *Commun. Eng.* **4**, 104 (2025).
17. Orfanoudakis, S. et al. Scalable reinforcement learning for large-scale coordination of electric vehicles using graph neural networks. *Commun. Eng.* **4**, 118 (2025).
18. Deng, J. et al. ImageNet: A large-scale hierarchical image database. In *Proc. IEEE Conference on Computer Vision and Pattern Recognition* 248–255 (2009).
19. Zamzmi, G. et al. Scorecard for synthetic medical data evaluation. *Commun. Eng.* **4**, 130 (2025).
20. Griffin, M. R. et al. 3D vector field-guided toolpathing for 3D bioprinting. *Commun. Eng.* **4**, 154 (2025).
21. Ahmed, K., Jiang, X., Ashraf, G. & Qiang, X. Freeze–thaw recycling for fiber–resin separation in retired wind blades. *Commun. Eng.* **4**, 153 (2025).
22. Sinha, S. K. & Fieguth, P. W. Segmentation of buried concrete pipe images. *Autom. Constr.* **15**, 47–57 (2006).
23. Parker, T., Shatalin, S. & Farhadiroushan, M. Distributed acoustic sensing—a new tool for seismic applications. *First Break* **32**, 61–69 (2014).
24. Tan, D. Y. et al. Real-time monitoring of water states in large-diameter aqueducts—learning from distributed acoustic sensing signals. *Commun. Eng.* **4**, 156 (2025).
25. Tilloy, A., Malamud, B. D., Winter, H. & Joly-Laugel, A. A review of quantification methodologies for multi-hazard interrelationships. *Earth Sci. Rev.* **196**, 102881 (2019).
26. Crosti, C., Duthinh, D. & Simiu, E. Risk consistency and synergy in multihazard design. *J. Struct. Eng.* **137**, 844–849 (2011).
27. Hadlos, A., Opdyke, A. & Hadigheh, S. Optimising housing typology distributions for multi-hazard loss reductions in resource-constrained settings. *Commun. Eng.* **4**, 175 (2025).
28. Wang, C. et al. StarWhisper Telescope: an AI framework for automating end-to-end astronomical observations. *Commun. Eng.* **4**, 184 (2025).
29. Zou, Y. et al. Enabling multirotor UAVs to perch, land and detach with standard propeller guards. *Commun. Eng.* **4**, 185 (2025).
30. Nahon, D. et al. Standardizing designed and emergent quantitative features in microphysiological systems. *Nat. Biomed. Eng.* **8**, 941–962 (2024).
31. C. Olaizola-Rodrigo, C. et al. A review of organ-on-chip fabrication methods: From early developments to overcoming inert barriers. *iScience* **28**, 113992 (2025).
32. Goswami, I. et al. Pillar arrays as tunable interfacial barriers for microphysiological systems. *Commun. Eng.* **4**, 197 (2025).
33. Alipour Bonab, S. et al. Advanced deep-learning model for temporal-dependent prediction of dynamic behavior of AC losses in superconducting propulsion motors for hydrogen-powered cryo-electric aircraft. *Commun. Eng.* https://doi.org/10.1038/s44172-025-00554-8 (2025).

Competing interests

The authors declare no competing interests.